Available online at www.sciencedirect.com
ScienceDirect
Journal of Sound and Vibration 320 (2009) 145–162
JOURNAL OF SOUND AND VIBRATION
www.elsevier.com/locate/jsvi

Analysis of forced transient response for rotating tires using REF models

Y.T. Wei[a,*], L. Nasdala[b], H. Rothert[b]

[a]State Key Laboratory of Automotive Safety and Energy, Tsinghua University, Beijing 100084, PR China
[b]Institute for Structural Analysis, University of Hannover, Appelstr. 9A, 30167 Hannover, Germany

Received 2 July 2008; accepted 12 July 2008
Handling Editor: L.G. Tham
Available online 6 September 2008

Abstract

This paper presents a new approach for tire dynamic analysis. By using this method, transient response for rotating tires under various loading situations can be analyzed. The well-known model of ring on elastic foundations (REF) is utilized to model tires. The general forced solution of undamped inextensible vibration is derived by the use of a modal expansion technique as well as Meirovitch modal analysis method. Closed form transient response for the stationary constant point load case is obtained; for the case of damped vibration, the response of rotating tire is formulated by using the first-order matrix perturbation theory together with Meirovitch modal analysis method. The effects of damping on the tire response are investigated. The developed method has been validated by comparison with direct numerical integration results. Combined with a contact or interface model, the proposed methodology can be used to model the tire dynamic responses under any given road profile.

1. Introduction

Pneumatic tires greatly influence the riding comfort and noise level in cars. The dynamic response of tires, hence, has been investigated since the early 1960s. Experimental natural frequencies and modes of tires have been studied by Chiesa [1], Böhm [2], Potts et al. [3], and Guan and her co-workers [4–6]. Theoretical efforts range from approximating the tire as a tension band, through treating it as a ring on an elastic foundation, to a finite element approach [7–29]. Of these, the ring on elastic foundations (REF) model (see Fig. 1) has been the most frequently adopted [7–20] because of the completeness and simplicity of ring theory yet with less sacrifice of result accuracy.

The REF model of tires was initially developed by Clark [7], Tielking [8], Böhm [2] etc. in the 1960s to study tire dynamic stiffness and tire–road contact problems. In their early work, tire sidewall was treated as radial springs only and without considering initial stress, rotating, and wheel effects. Pacejia [10] first introduced both radial and tangential springs to model the tire sidewall. Padovan [9] introduced treadband and sidewall

*Corresponding author. Tel.: +86 10 62797400x5005; fax: +86 10 62785708.
E-mail address: weiyt@mail.tsinghua.edu.cn (Y.T. Wei).

0022-460X/$ - see front matter © 2008 Elsevier Ltd. All rights reserved.
doi:10.1016/j.jsv.2008.07.007

Nomenclature

A	ring section area
$a_n(t)$, $b_n(t)$	generalized coordinates
b	ring width
c_w, c_v	distributed damping coefficients of sidewall in radial and tangential directions, respectively
EA	membrane stiffness of the ring
EI	bending stiffness of the ring
f_n	natural frequency (Hz)
k_w, k_v	distributed springs of sidewall in radial and circumferential directions, respectively
h	ring thickness
n	mode number
(r, θ)	mean radius and ring coordinates in the rotating coordinate system, respectively
p_0	internal pressure
p_{nk}	modal participation factors
q_w, q_v, q_β	applied radial, tangential force and moment, respectively
(r, ϕ)	mean radius and ring coordinates in the non-rotating coordinate system, respectively
U, T, W	potential, kinetic, and external force energy respectively
v, w	represent the mid-plane displacements of the ring
$\bar{v}, \bar{w}$	circumferential and radial displacements of the ring
(x, z)	Cartesian coordinates in the non-rotating coordinate system
(x^*, z^*)	Cartesian coordinates in the rotating coordinate system
$(\ )'$	(prime) designates the differentiation with respect to θ
ρ	density
σ_θ^0	initial stress in the ring
ω_{nk}	natural frequencies (rad/s)
Ω	rotation speed
$(\dot{})$	(dot) indicates the differentiation with respect to time

damping and Potts et al. [3] added rotating effect into the ring model. Initial stress effect was also addressed by Pacejka [10], Padovan [9], and Potts et al. [3]. Using ring-type model, Gong [18] investigated the dynamic properties of tire–wheel system in detail, especially the transfer characteristics of the system and Dohrmann [19] studied the dynamics of the tire–wheel-suspension system. More recently, so-called the rigid ring model [30] and the flexible ring model [31] were used to establish the tire model for Noise Vibration and Harshness

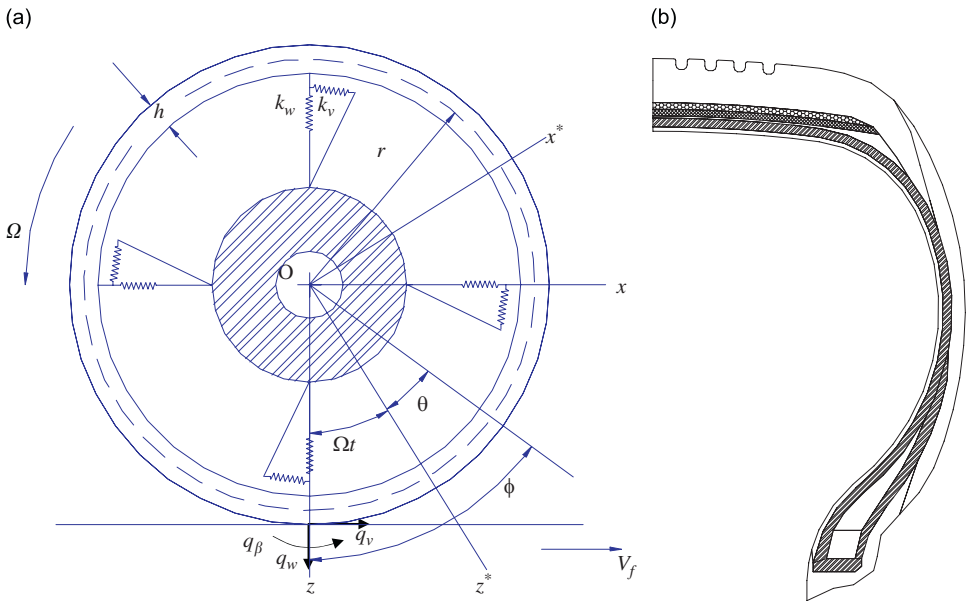

Fig. 1. Schematic of tire ring model and tire section structure: (a) tire ring model and (b) tire section structure.

(NVH) and ride comfort simulations. Huang and co-workers [16,17] derived the general equations of motion that govern both transverse and circumferential motions of rotating rings and expanded the solution to forced response. Several authors [18–20] investigated the forced response of the REF model under various loading situations by modal expansion method.

The purpose of this paper is to present an analytical formulation of complete forced solution including transient response for rotating tire REF model under various loading conditions. Following the introduction we give, in Section 2, the equations of motion of a general rotating tire ring model using Hamilton principle. In Section 3, the natural frequencies are obtained by using mode techniques. Then the physical parameters are determined by fitting the predicted natural frequencies to the measured ones. In Section 4, the general forced solution of undamped inextensible vibration is formulated by making use of the modal expansion technique. Meirovitch modal analysis method [32,33] is then used to deal with the gyroscopic properties of the linear differential equations about the generalized coordinates. A closed form transient response for the stationary constant point load case is obtained. In Section 5, the response to damped vibration is investigated. The first-order perturbation theory and Meirovitch modal analysis [34] are used to solve the linear gyroscopic system about the generalized coordinates. Section 6 gives the summary and conclusions.

2. The equations of motion

In the case of a rotating tire modeled by a rotating ring on an elastic foundation as shown in Fig. 1, the elastic properties of the sidewall are modeled by distributed springs, k_w and k_v, in radial and circumferential directions, respectively. In order to describe the dynamics of the rotating ring it is convenient to have a coordinate system that rotates with the wheel body. In contrast, the analysis of contact deformation and forces is more conveniently performed using a separate coordinate system that translates with the contact patch of the tire [18–20]. The origins of both coordinate systems are at the center of the wheel. The location of an element of the tire is described using polar coordinates (r, ϕ) in the non-rotating coordinate system, or (r, θ) in the rotating coordinate system. As seen in Fig. 1, the angular coordinates originate from the vertical axis pointing downward through the wheel center and are taken as positive in the counter-clockwise direction. The locations can also be expressed as Cartesian coordinates either (x, z) in the non-rotating coordinate system, or (x^*, z^*) in the rotating coordinate system. The x-axis is positive in the direction of the forward velocity, and the z-axis is positive in the downward direction.

According to thin shell assumption, the flexural strain of the ring can be written as

$$\varepsilon_\theta = \frac{\bar{v}' + \bar{w}}{r} + \frac{1}{2}\left(\frac{\bar{v}' + \bar{w}}{r}\right)^2 + \frac{1}{2}\left(\frac{\bar{v} - \bar{w}'}{r}\right)^2 \tag{1}$$

where r and θ are the mean radius and ring coordinates, respectively, $\bar{v}$ and $\bar{w}$ represent circumferential and radial displacements of the ring, and primes designate the differentiation with respect to θ. Note that the nonlinear term has to be included in the strains in order to compute the initial stress work correctly [16–18].

Inserting the expressions $\beta = (v - w'/r), \bar{v} = v + z\beta$, and $\bar{w} = w$, where v and w represent the mid-plane displacements, into Eq. (1) yields

$$\varepsilon_\theta = \frac{v' + w}{r} + \frac{1}{2}\left(\frac{v' + w}{r}\right)^2 + \frac{1}{2}\left(\frac{v - w'}{r}\right)^2 + \frac{z}{r^2}(v' - w'') \tag{2}$$

The Hamilton principle is used to derive the equations of motion. Then all the energies can be expressed as follows:

$$U = b\int_0^{2\pi}\int_{-(h/2)}^{(h/2)}\left[\frac{1}{2}\sigma_\theta\varepsilon_\theta + \sigma_\theta^0\varepsilon_\theta\right] r\,\mathrm{d}z\,\mathrm{d}\theta + \int_0^{2\pi}\left[\frac{1}{2}k_w w^2 + \frac{1}{2}k_v v^2\right] r\,\mathrm{d}\theta \tag{3a}$$

$$T = \int_0^{2\pi}\frac{1}{2}\rho A r((\dot{w} - \Omega v)^2 + (\dot{v} + \Omega(w + r))^2)\,\mathrm{d}\theta \tag{3b}$$

$$W = p_0 r \int_0^{2\pi} \left[w + \frac{1}{2r}(v^2 - vw' + v'w + w^2) \right] \mathrm{d}\theta + \int_0^{2\pi} \left(q_w w + q_\theta v + q_\beta \frac{v' - w}{r} \right) r \, \mathrm{d}\theta \tag{3c}$$

where U, T, and W are potential, kinetic, and external force energy, respectively, ρ the density, b the ring width, p_0 the internal pressure, A the ring section area which is the product of ring width b and the belt effective thickness, k the elastic constant of foundation, h the ring thickness, q_w, q_v, and q_β the applied radial, tangential force, and moment, respectively, Ω the rotation speed, and σ_θ^0 denotes the initial stress given by

$$\sigma_\theta^0 A = \frac{1}{2} \int_0^{\pi} (\rho A \Omega^2 r + p_0 b) \sin\theta r \, \mathrm{d}\theta = p_0 b r + \rho A r^2 \Omega^2 \tag{4}$$

Hamilton principle can be expressed as

$$\delta \int_{t_1}^{t_2} [U - T - W] \, \mathrm{d}t = 0 \tag{5}$$

Substituting Eqs. (2)–(4) into Eq. (5), and rearranging the terms yields the final equations of motion

$$\begin{aligned} &-\frac{EI}{r^4}(v^6 + 2v^4 + v'') + \sigma_\theta^0 A \frac{1}{r^2}(v^4 + 2v'' + v) - k_w v'' + k_v - p_0 b \frac{1}{r}(v + v'') \\ &\quad + \rho A(\ddot{v} - \ddot{v}'' - 4\Omega \dot{v}' + \Omega^2(v'' - v)) = q_w' + q_v + \frac{1}{r} q_\beta'' + \frac{1}{r} q_\beta \end{aligned} \tag{6}$$

where the inextensible condition, i.e., $v' + w = 0$, is used. In Eq. (6), E is effective modulus of the belt and I the moment of inertia, which means EI is the effective bending stiffness of the ring.

3. Parameters identification

As suggested by Gong [18], the natural frequencies of the non-rotating tires are used to determine the model parameters and validate the model. With Ω, q_w, q_v and q_β being set to zero, Eq. (6) can be written as

$$-\frac{EI}{r^4}(v^6 + 2v^4 + v'') + \frac{p_0 b}{r}(v^4 + v'') - k_w v'' + k_v + \rho A(\ddot{v} - \ddot{v}'') = 0 \tag{7}$$

Assume the free vibration mode in the sinusoidal series as follows:

$$v(\theta, t) = \sum_{n=0}^{\infty} A_n \sin(n\theta + \omega_n t) \tag{8}$$

Inserting Eq. (8) into Eq. (7) yields the following natural frequency expression:

$$f_n = \frac{\omega_n}{2\pi} = \frac{1}{2\pi} \left\{ \frac{1}{\rho A(1 + n^2)} \left(\frac{EI}{r^4}[n^6 - 2n^4 + n^2] + \frac{p_0 b}{r}[n^4 - n^2] + k_w n^2 + k_v \right) \right\}^{1/2} \tag{9}$$

By matching the natural frequencies predicted by Eq. (9) with the measured ones, the model physical parameters, including k_w, k_v and EI are determined. The geometrical and structural model parameters, including ρ, A, b, r and h, are obtained directly from the tire design. For a type of radial tire, 195/70R14, the geometrical and structural model parameters are listed in Table 1.

Table 2 lists the natural frequencies up to the eighth mode of this tire obtained from experimental modal analysis and theoretical prediction by Eq. (9). Through analyzing the experimental mode shape corresponding to each natural frequencies, we know that rank 1 corresponds to $n = 2$, rank 2 to $n = 3$ and rank 8 to $n = 8$. Substituting the natural frequencies of $n = 2$, 3, 8 in Eq. (9), and then solving for the model physical parameters leads to $k_w = 1.64 \times 10^6\,\mathrm{N/m^2}$, $k_v = 2.19 \times 10^5\,\mathrm{N/m^2}$, $EI = 1.41\,\mathrm{N\,m^2}$. Substituting the obtained physical parameters into Eq. (9) yields all natural frequencies. As for $n = 2$, 3, 8, the predictions and experiments agree exactly, as expected. For $n = 4$–7, maximum error is only 0.92%. The good agreement between the predictions and experiments, to a certain extent, validates the model.

Table 1
Model geometrical and structural parameters of a 195/70R14 radial tire

Parameters type	Unit	Numerical value
b	m	0.16
h	m	0.01
A	m^2	0.0016
p_0	N/m^2	2.5×10^5
ρ	kg/m^3	2.28×10^3
r	m	0.285

Table 2
Tire natural frequencies: experimental vs. REF model

Rank	$n=0$	$n=1$	$n=2$	$n=3$	$n=4$	$n=5$	$n=6$	$n=7$	$n=?$	$n=8$
f_n: Experimental	–	–	108.53	132.38	158.30	186.92	213.60	248.14	255.36	278.54
f_n: REF model	39.01	80.39	108.53	132.38	157.83	185.36	214.78	245.88	–	278.54

4. General forced response of undamped rotating REF

4.1. Derivation of forced solution

While natural frequencies and modes provide important information for understanding the system, of more interest is the response to certain types of forces. The forced response of the tangential displacement of the ring to any arbitrary forcing function is therefore assumed to be of the form [17,18,20]

$$v = \sum_{n=1}^{\infty} \sum_{k=1}^{2} [p_{nk} \sin(n\theta + \omega_{nk} t)] \tag{10}$$

where ω_{nk} are the natural frequencies, n the mode number, and p_{nk} the modal participation factors, which are unknown and depend on the applied forces. The above expression can be rearranged as

$$v = \sum_{n=1}^{\infty} [a_n(t) \cos n\theta + b_n(t) \sin n\theta] \tag{11}$$

where $a_n(t)$ and $b_n(t)$ are the generalized coordinates defined as

$$a_n(t) = \sum_{k=1}^{2} p_{nk}(t) \sin(\omega_{nk} t), \quad b_n(t) = \sum_{k=1}^{2} p_{nk}(t) \cos(\omega_{nk} t) \tag{12}$$

Substituting Eq. (11) into Eq. (6) and making use of the orthogonality of $\sin(n\theta)$ and $\cos(n\theta)$, the motion of the tire ring model in the generalized coordinates $a_n(t)$ and $b_n(t)$ reduces to a set of linear second-order ordinary differential equations

$$\begin{bmatrix} m_n & \\ & m_n \end{bmatrix} \begin{Bmatrix} \ddot{a}_n \\ \ddot{b}_n \end{Bmatrix} + \begin{bmatrix} 0 & g_n \\ -g_n & 0 \end{bmatrix} \begin{Bmatrix} \dot{a}_n \\ \dot{b}_n \end{Bmatrix} + \begin{bmatrix} k_n & \\ & k_n \end{bmatrix} \begin{Bmatrix} a_n \\ b_n \end{Bmatrix} = \begin{Bmatrix} \xi_n \\ \zeta_n \end{Bmatrix} \tag{13}$$

where

$$k_n = \left(\frac{EI}{R^4} n^2 + \frac{\sigma_\theta^0}{R^2} \right) (1 - n^2)^2 + k_v + k_w n^2 - \frac{p_0 b}{R} (1 - n^2) - \rho A (1 + n^2) \Omega^2, \quad m_n = \rho A (1 + n^2),$$

and $g_n = -4\rho A n \Omega$.

The generalized force corresponding to physical force and moments are

$$\left\{\begin{array}{l}\xi_n=\dfrac{1}{\pi}\int\left(q_v+q'_w+\frac{1}{R}(q_\beta+q''_\beta)\right)\cos\, n\theta\,\mathrm{d}\theta\\ \zeta_n=\dfrac{1}{\pi}\int\left(q_v+q'_w+\frac{1}{R}(q_\beta+q''_\beta)\right)\sin\, n\theta\,\mathrm{d}\theta\end{array}\right\} \tag{14}$$

Eq. (13) can be written in the matrix form

$$\mathbf{M}\ddot{\mathbf{y}}+\mathbf{G}\dot{\mathbf{y}}+\mathbf{K}\mathbf{y}=\mathbf{Q} \tag{15}$$

where

$$\mathbf{y}=\begin{bmatrix}a_n & b_n\end{bmatrix}^{\mathrm{T}},\quad \mathbf{M}=\begin{bmatrix}m_n & \\ & m_n\end{bmatrix},\quad \mathbf{G}=\begin{bmatrix} & g_n\\ -g_n & \end{bmatrix},\quad \mathbf{K}=\begin{bmatrix}k_n & \\ & k_n\end{bmatrix}\quad\text{and}\quad \mathbf{Q}=\begin{Bmatrix}\xi_n\\ \zeta_n\end{Bmatrix}$$

It is seen that matrix $\mathbf{G}$ is skew-symmetric, $\mathbf{G}^{\mathbf{T}}=-\mathbf{G}$, and matrix $\mathbf{M}$ and $\mathbf{K}$ are symmetric, $\mathbf{M}^{\mathrm{T}}=\mathbf{M}$, $\mathbf{K}^{\mathrm{T}}=\mathbf{K}$. Eq. (15) can be interpreted as a linear gyroscopic system with two degrees of freedom. Meirovitch [33] has developed a closed form solution for such system in a manner similar to classical modal analysis.

4.2. Analysis of response using Meirovitch method

The second0-order differential Equation (15) can be written in state space form as follows:

$$\begin{bmatrix}\mathbf{M} & \\ & \mathbf{K}\end{bmatrix}\dot{\mathbf{x}}+\begin{bmatrix}\mathbf{G} & \mathbf{K}\\ -\mathbf{K} & 0\end{bmatrix}\mathbf{x}=\begin{Bmatrix}\mathbf{Q}\\ 0\end{Bmatrix} \tag{16}$$

or

$$\mathbf{I}\dot{\mathbf{x}}(t)+\mathbf{G}^{*}\mathbf{x}(t)=\bar{\mathbf{Q}} \tag{17}$$

where $\mathbf{x}=[\dot{\mathbf{y}}^{\mathrm{T}}\quad \mathbf{y}^{\mathrm{T}}]^{\mathrm{T}}$ is the state vector and $\bar{\mathbf{Q}}$ the generalized force vector. Meirovitch [33] developed a modal analysis method to obtain the closed form solution of Eq. (17). This method is especially designed to permit the treatment of gyroscopic system of the type described by Eqs. (15) or (17). According to Meirovitch method, the complete solution for the state vector of Eq. (17) can be obtained as follows:

$$\begin{aligned}\mathbf{x}(t)=\sum_{r=1}^{n}\Bigg\{\int_0^t\left[(\mathbf{y}_r\mathbf{y}_r^{\mathrm{T}}+\mathbf{z}_r\mathbf{z}_r^{\mathrm{T}})\bar{\mathbf{Q}}(\tau)\cos\,\omega_r(t-\tau)+(\mathbf{y}_r\mathbf{z}_r^{\mathrm{T}}-\mathbf{z}_r\mathbf{y}_r^{\mathrm{T}})\bar{\mathbf{Q}}(\tau)\sin\,\omega_r(t-\tau)\right]\mathrm{d}\tau\Bigg\}\\ +[(y_ry_r^{\mathrm{T}}+z_rz_r^{\mathrm{T}})\mathbf{I}\mathbf{x}(0)\cos\omega_rt+(\mathbf{y}_r\mathbf{z}_r^{\mathrm{T}}-\mathbf{z}_r\mathbf{y}_r^{\mathrm{T}})\mathbf{I}\mathbf{x}(0)\sin\,\omega t]\end{aligned} \tag{18}$$

which represents the response to any excitation forces and initial disturbances. In Eq. (18), $\mathbf{y}_r$ and $\mathbf{z}_r$ are real and imaginary part of the eigenvector of the system, as shown in Table 3.

4.3. Forced response of undamped rotating REF

In order to make use of Eq. (18) to obtain the solution of Eq. (15), one must first solve the eigenvalues and eigenfunctions of state equation (17). To this end, the matrices $\mathbf{I}$ and $\mathbf{G}^{*}$ with order 4×4 are written as follows:

$$\mathbf{I}=\begin{bmatrix}\mathbf{M} & \\ & \mathbf{K}\end{bmatrix},\quad \mathbf{G}^{*}=\begin{bmatrix}\mathbf{G} & \mathbf{K}\\ -\mathbf{K} & \mathbf{0}\end{bmatrix} \tag{19}$$

Because the matrices $\mathbf{I}$ and $\mathbf{G}^{*}$ are already specified, now the eigenvalue problem corresponding to Eq. (17) can be solved. Table 3 shows the solution of this eigenvalue problem which consists of two pairs of repeated eigenvalues ω_r^2 and t pairs of associated eigenvectors $\mathbf{y}_r$ and $\mathbf{z}_r$.

It is seen that the eigenvalues obtained here, ω_r, $r=1,2$, are identical with the natural frequencies of rotating tire REF model by Gong [18] or Dohrmann [19]. Inserting the obtained eigenvalues ω_r, $r=1,2$, and

Table 3
Eigenvalues and eigenfunctions of the linear gyroscopic system (Eq. (17))

$$\omega_{1,2}^2 = \left\{ \frac{g^2+2km-gCg^2+2km+gC}{2m^2} \quad \frac{}{2m^2} \right\}$$

$$\mathbf{z}_1 = \left\{ \frac{-g+C}{2\sqrt{kmA}} \quad 0 \quad 0 \quad \frac{1}{\sqrt{A}} \right\}$$

$$\mathbf{z}_2 = \left\{ \frac{-g-C}{2\sqrt{kmB}} \quad 0 \quad 0 \quad \frac{1}{\sqrt{B}} \right\}$$

$$\mathbf{y}_1 = \left\{ 0 \quad \frac{g-C}{2\sqrt{kmA}} \quad \frac{1}{\sqrt{A}} \quad 0 \right\}$$

$$\mathbf{y}_2 = \left\{ 0 \quad \frac{g+C}{2\sqrt{kmB}} \quad \frac{1}{\sqrt{B}} \quad 0 \right\}$$

where

$$A = 1 + \frac{(g-\sqrt{g^2+4km})^2}{4km}$$

$$B = 1 + \frac{(g+\sqrt{g^2+4km})^2}{4km}$$

$$C = \sqrt{g^2+4km}$$

eigenvectors $\mathbf{y}_r$ and $\mathbf{z}_r$, $r = 1,2$ into Eq. (18) results in the formulation of response for undamped vibration of rotating rings to any excitation forces and initial disturbances. As an example, the forced response of the undamped rotating REF for stationary constant point load is investigated according to the developed procedure. The closed form solution for transient response of the model is obtained.

The generalized force vector $\{\mathbf{Q}^{\mathrm{T}} \quad 0\}^{\mathrm{T}}$ of Eq. (16) for the case of a concentrated transverse load is first evaluated. By referring to Fig. 1, the stationary point load on the rotating ring can be described as

$$q_w = \left(\frac{-f}{r}\right)\delta(\theta - (\phi_0 - \Omega t)), \quad q_v = q_\beta = 0 \tag{20}$$

where f is the applied force per unit width and minus sign indicates the force direction opposite to the positive transverse displacement, ϕ_0 is the initial point load location at a time equal to zero. The generalized force vector of Eq. (17) therefore becomes

$$\bar{\mathbf{Q}}(t) = \left\{ -\frac{nf}{\pi r}\sin n(\phi_0 - \Omega t) \quad \frac{nf}{\pi r}\cos n(\phi_0 - \Omega t) \quad 0 \quad 0 \right\}^{\mathrm{T}} \tag{21}$$

Introducing Eq. (21), the eigenvalues ω_r, $r = 1,2$, and eigenvectors $\mathbf{y}_r$ and $\mathbf{z}_r$, $r = 1,2$ described in Table 3, into Eq. (18) and then making use of Eq. (11) yields the closed form tangential displacement response as follows:

$$v(\theta,t) = -\sum_{n=1}^{\infty} nf\left[\frac{\sin n\phi - ((1/2)+\bar{A})\sin(n\phi+\hat{\omega}_{n1}t) - ((1/2)-\bar{A})\sin(n\phi+\hat{\omega}_{n2}t)}{\pi(m_n n^2\Omega^2 + g_n n\Omega - k_n)}\right] \tag{22}$$

where

$$\phi = \theta + \Omega t, \quad \bar{A} = \frac{\rho A n(n^2-1)\Omega}{\sqrt{g_n^2+4k_n m_n}}$$

and $\hat{\omega}_{n1,2} = \omega_{n1,2} - n\Omega$ are the natural frequencies of the system in the fixed reference frame (see Ref. [19]).

The transverse displacements can be determined according to the relation, $v' + w = 0$, as follows:

$$w(\theta,t) = \sum_{n=1}^{\infty} n^2 f\left[\frac{\cos n\phi - ((1/2)+\bar{A})\cos(n\phi+\hat{\omega}_{n1}t) - ((1/2)-\bar{A})\cos(n\phi+\hat{\omega}_{n2}t)}{\pi(m_n n^2\Omega^2 + g_n n\Omega - k_n)}\right] \tag{23}$$

It is seen that the solutions (22) and (23) include not only steady but also transient response. The steady solutions for tangential and transverse displacements are, respectively, as follows:

$$v(\theta,t) = -\sum_{n=1}^{\infty}\left[nf\ \sin n\phi/\pi(m_n n^2\Omega^2 + g_n n\Omega - k_n)\right] \tag{24}$$

$$w(\theta,t) = \sum_{n=1}^{\infty}\left[\frac{n^2 f\ \cos n\phi}{\pi(m_n n^2\Omega^2 + g_n n\Omega - k_n)}\right] \tag{25}$$

By integrating the distributed forces in the sidewall springs the wheel center load is obtained as

$$F_{\text{axle}} = -f\{1 - \cos(\hat{\omega}_1 t)\} \tag{26}$$

where the orthogonality of trigonometric functions is used.

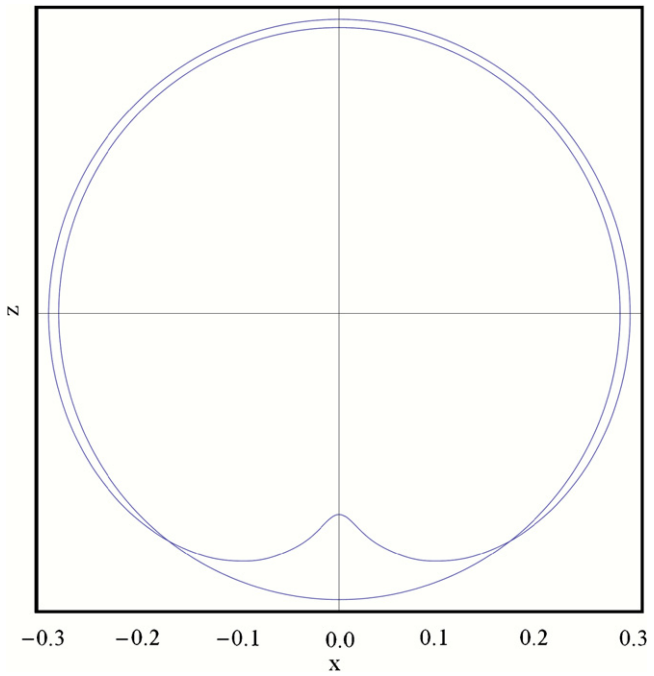

Fig. 2. Schematic of steady radial deformation (m) configuration, $\Omega = 200$ rad/s: undamped.

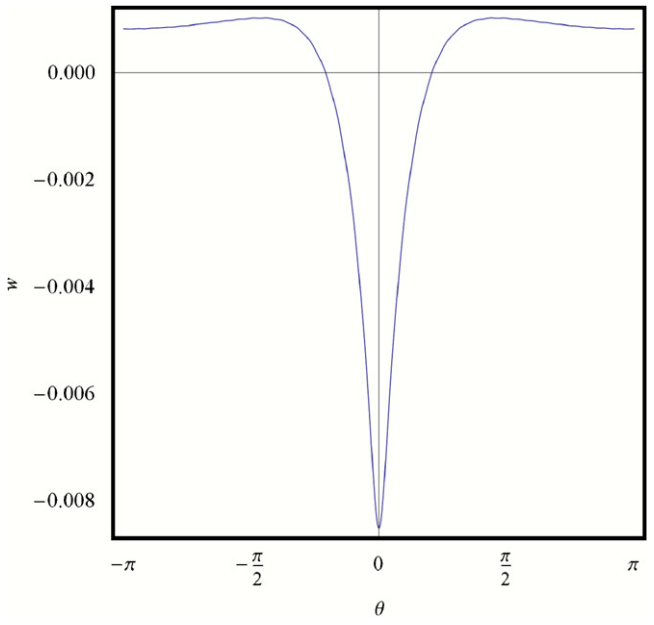

Fig. 3. Steady radial deformation (m) along the circumference (radian), $\Omega = 200$ rad/s: undamped.

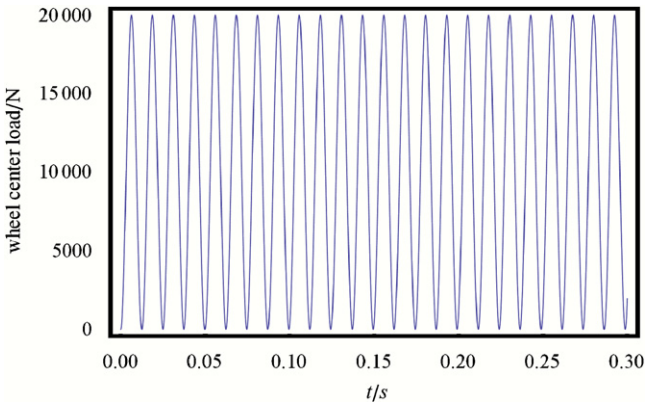

Fig. 4. Variation of wheel center load (N) with time (s), $\Omega = 200$ rad/s: undamped.

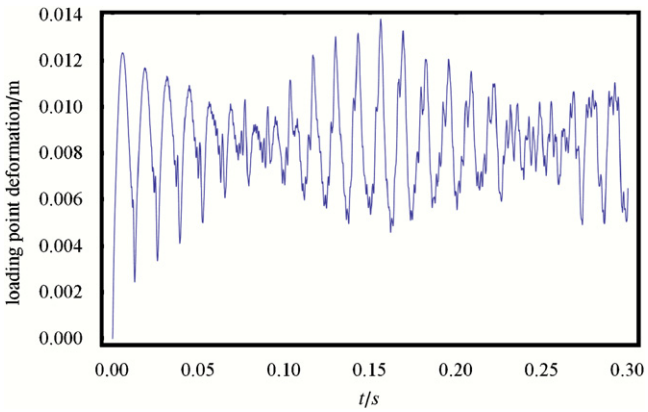

Fig. 5. Variation of radial deformation (m) at loading point with time (s), $\Omega = 200$ rad/s: undamped.

Note that in the above equation $\hat{\omega}_1 = \sqrt{(k_w + k_v)/2\rho A}$ is independent of the rotating speed. It can be seen that the wheel center load behaves like a vibration system with one degree of freedom whose vibration frequency is independent of rotating speed and equal to the first-order natural frequency of non-rotating rings. Because the parameters of tire ring model are already specified previously, given applied force f (here $f = 10\,000$ N) we can give numerical results of the tire response including wheel center load and tire displacements, some of which are graphically shown in Figs. 2–5. It is seen that the tire displacements at the loading point contain multiple frequencies (see Fig. 5) in contrast with the wheel center load (see Fig. 4).

5. General forced response of damped rotating REF

5.1. The equations of motion for damped rotating REF

In the case of damped vibration, the tire is modeled as a ring on viscoelastic foundation with distributed springs, k_w and k_v, and damping coefficients, c_w and c_v, in the radial and tangential directions respectively [19,20]. The equations of motion (6) therefore are modified as

$$-\frac{EI}{r^4}(v^6 + 2v^4 + v'') + \sigma_\theta^0 A\frac{1}{r^2}(v^4 + 2v'' + v) - k_w v'' + k_v v - c_w \dot{v}'' + c_v \dot{v} - p_0 b\frac{1}{r}(v + v'')$$
$$+ \rho A(\ddot{v} - \ddot{v}'' - 4\Omega\dot{v}' + \Omega^2(v'' - v)) = q_w' + q_v + \frac{1}{r}q_\beta'' + \frac{1}{r}q_\beta \tag{27}$$

The actual damping characteristics of a complex system such as the tire are very difficult to model precisely. For the sake of simplification, the linear viscoelastic elements are included in the viscoelastic foundation. Kim and Savkoor [20] investigated the effects of different damping models on the tire steady behaviors (contact pressure distribution, rolling resistance).

Substituting Eq. (11) into Eq. (27) and making use of the orthogonality of $\sin(n\theta)$ and $\cos(n\theta)$ yields the motion of the damped tire ring model in the generalized coordinates $a_n(t)$ and $b_n(t)$

$$\mathbf{M}\ddot{\mathbf{y}} + [\mathbf{G} + \mathbf{C}]\dot{\mathbf{y}} + \mathbf{K}\mathbf{y} = \mathbf{Q} \tag{28}$$

where

$$\mathbf{M} = \begin{bmatrix} m_n & \\ & m_n \end{bmatrix}, \quad \mathbf{G} = \begin{bmatrix} & g_n \\ -g_n & \end{bmatrix}, \quad \mathbf{C} = \begin{bmatrix} c_n & \\ & c_n \end{bmatrix}, \quad \mathbf{K} = \begin{bmatrix} k_n & \\ & k_n \end{bmatrix}, \quad \text{and} \quad \mathbf{Q} = \begin{Bmatrix} \xi_n \\ \zeta_n \end{Bmatrix}$$

In the state space, Eq. (28) can be rewritten as

$$\mathbf{I}\dot{\mathbf{x}}(t) + \mathbf{G}^*\mathbf{x}(t) = \bar{\mathbf{Q}} \tag{29}$$

where

$$\mathbf{I} = \begin{bmatrix} \mathbf{M} & \\ & \mathbf{K} \end{bmatrix}, \quad \mathbf{G}^* = \begin{bmatrix} \mathbf{G}+\mathbf{C} & \mathbf{K} \\ -\mathbf{K} & \mathbf{0} \end{bmatrix}, \quad \bar{\mathbf{Q}} = \begin{bmatrix} \mathbf{Q} \\ \mathbf{0} \end{bmatrix}, \quad c_n = c_v + c_w n^2 \tag{30}$$

The viscous damping coefficients, c_w and c_v, are difficult to determine directly for a given tire; however, the damping coefficients c_n can be deduced from the measured modal damping coefficients, ζ_n, from the relationship $c_n = 2\zeta_n\sqrt{k_n m_n}$.

Eq. (29) can be interpreted as a linear damped gyroscopic system [34] with two degrees of freedom. The problem of damped gyroscopic system is considerably more complicated than those corresponding to undamped gyroscopic, damped or undamped natural system cases. The sum of the damping matrix and the gyroscopic matrix, i.e., $\mathbf{G}^*$ is an arbitrary matrix. Hence, any advantage resulting from the symmetry or skew-symmetry of coefficient matrices is lost, so that one must return to the general theory. However, in the case of small damping, the damping can be regarded as a perturbation to the unperturbed gyroscopic system. A first-order perturbation theory is adopted to obtain the solution for the response of slightly damped gyroscopic systems, e.g., the rotating ring model state equation (29), in this paper.

5.2. System response solution based on perturbation theory of matrix [34]

In the case of slightly damped gyroscopic systems such as Eqs. (28) or (29), the matrix $\mathbf{C}$ can be regarded as being of one order of magnitude smaller than matrix $\mathbf{G}$ and $\mathbf{K}$. Hence, one can rewrite Eq. (29) as

$$\dot{\mathbf{X}}(t) + \mathbf{A}\mathbf{X}(t) = \tilde{\mathbf{U}} \tag{31}$$

where

$$\mathbf{I} = \mathbf{L}\mathbf{L}^{\mathrm{T}}, \quad \mathbf{A} = \mathbf{A}_0 + \mathbf{A}_1, \quad \mathbf{A}_0 = \mathbf{L}^{-1}\begin{bmatrix} \mathbf{G} & \mathbf{K} \\ -\mathbf{K} & \mathbf{0} \end{bmatrix}\mathbf{L}^{-\mathrm{T}}, \quad \mathbf{A}_1 = \mathbf{L}^{-1}\begin{bmatrix} \mathbf{C} & \mathbf{0} \\ \mathbf{0} & \mathbf{0} \end{bmatrix}\mathbf{L}^{-\mathrm{T}}, \quad \tilde{\mathbf{U}} = \mathbf{L}^{-1}\overline{\mathbf{Q}}\mathbf{L}^{-\mathrm{T}}$$

The symmetry and skew-symmetry of $\mathbf{A}_1$ and $\mathbf{A}_0$, respectively, are readily apparent. Because matrix $\mathbf{A}_1$ is one order of magnitude smaller than $\mathbf{A}_0$, the theory of first-order perturbation of matrix is applicable. Based on the formulation for response of general damped gyroscopic systems [34] and the first-order perturbation solution for slightly damped gyroscopic system, the system response of Eq. (29) can be obtained as follows:

$$\begin{aligned}\begin{bmatrix} \dot{\mathbf{y}}(t) \\ \mathbf{y}(t) \end{bmatrix} = \mathbf{L}^{-\mathrm{T}} \sum_{i=1}^{n} \Bigg\{ & \mathrm{e}^{-\lambda_{1i}t} \cos\,\omega_{0i}t \mathbf{R}_i \mathbf{L}^{\mathrm{T}} \begin{bmatrix} \dot{\mathbf{y}}(0) \\ \mathbf{y}(0) \end{bmatrix} + \mathrm{e}^{-\lambda_{1i}t} \sin\,\omega_{0i}t \mathbf{I}_i \mathbf{L}^{\mathrm{T}} \begin{bmatrix} \dot{\mathbf{y}}(0) \\ \mathbf{y}(0) \end{bmatrix} \\ & + \int_0^t \mathrm{e}^{-\lambda_{1i}(t-\tau)} \cos\,\omega_{0i}(t-\tau) \mathbf{R}_i \mathbf{L}^{-1} \begin{bmatrix} \bar{\mathbf{Q}}(\tau) \\ 0 \end{bmatrix} \mathrm{d}\tau + \int_0^t \mathrm{e}^{-\lambda_{1i}(t-\tau)} \sin\,\omega_{0i}(t-\tau) \mathbf{I}_i \mathbf{L}^{-1} \begin{bmatrix} \bar{\mathbf{Q}}(\tau) \\ 0 \end{bmatrix} \mathrm{d}\tau \Bigg\} \end{aligned} \tag{32}$$

where $\mathbf{R}_i$ and $\mathbf{I}_i$ are the respective real and imaginary parts of the $2n \times 2n$ matrix $\hat{\mathbf{y}}_i\hat{\mathbf{z}}_i^{\mathrm{T}}$, i.e.,

$$\hat{\mathbf{y}}_i\hat{\mathbf{z}}_i^{\mathrm{T}} = \mathbf{R}_i + i\mathbf{I}_i, \quad i = 1, 2, \ldots, 2n \tag{33}$$

in which $\hat{\mathbf{y}}_i$ and $\hat{\mathbf{z}}_i$ are the right and left eigenvectors of $\mathbf{A}$ respectively, λ_{1i} is the first correction of the eigenvalue of $\mathbf{A}$. Eq. (32) describes the response of the system in terms of real quantities alone. It should be pointed out that all the quantities for the evaluation of the first-order perturbations are computed by means of the eigenvalues and eigenvectors of the unperturbed system: i.e., those of an undamped gyroscopic system.

5.3. Formulation for response of damped vibration of rotating REF

Consider the two-degree of freedom, damped gyroscopic system Eq. (28) and its state expression Eq. (29). Eqs. (28) and (30) form the matrices $\mathbf{I}$ and $\mathbf{G}^*$:

$$\mathbf{I} = \begin{bmatrix} \mathbf{M} & \\ & \mathbf{K} \end{bmatrix} = \begin{bmatrix} m_n & & & \\ & m_n & & \\ & & k_n & \\ & & & k_n \end{bmatrix}, \quad \mathbf{G}^* = \begin{bmatrix} \mathbf{G}+\mathbf{C} & \mathbf{K} \\ -\mathbf{K} & 0 \end{bmatrix} = \begin{bmatrix} c_n & g_n & k_n & \\ -g_n & c_n & & k_n \\ -k_n & & 0 & \\ & -k_n & & 0 \end{bmatrix} \tag{34}$$

The Cholesky decomposition matrix $\mathbf{I}$, and its inverse, are

$$\mathbf{L} = \begin{bmatrix} \sqrt{m_n} & & & \\ & \sqrt{m_n} & & \\ & & \sqrt{k_n} & \\ & & & \sqrt{k_n} \end{bmatrix}, \quad \mathbf{L}^{-1} = \begin{bmatrix} 1/\sqrt{m_n} & & & \\ & 1/\sqrt{m_n} & & \\ & & 1/\sqrt{k_n} & \\ & & & 1/\sqrt{k_n} \end{bmatrix} \tag{35}$$

Following Eq. (31), one forms matrices $\mathbf{A}_0$, and $\mathbf{A}_1$:

$$\mathbf{A}_0 = \begin{bmatrix} 0 & g/m & \sqrt{k}/m & \\ -g/m & 0 & & \sqrt{k}/m \\ -\sqrt{k}/m & & 0 & \\ & -\sqrt{k}/m & & \end{bmatrix}, \quad \mathbf{A}_1 = \begin{bmatrix} c/m & & & \\ & c/m & & \\ & & 0 & \\ & & & 0 \end{bmatrix} \tag{36a,b}$$

Computations of the perturbations to the undamped eigensolutions proceed as indicated previously. The results are summarized in Table 4. One should note that the system eigenvalues and associated eigenvectors occur in complex conjugate pairs. Hence, one half of them are included. Furthermore, only the right eigenvectors are included.

The responses to the stationary constant point load f (here $f = 10000\,\mathrm{N}$) have been computed. Fig. 6 represents the steady deformation configuration of the model and Fig. 7 shows the steady radial deformation along the circumference. From Fig. 8 it is shown that the transient part of tire–wheel center load for the damped rotating ring model will be damped out eventually. As mentioned earlier,

Table 4
Eigenvalues and eigenfunctions of the linear damped gyroscopic system (Eq. (29))

λ_1	$\dfrac{-c(g^2+2km-gC)}{m(C^2-gC)}$	$\dfrac{-c(g^2+2km+gC)}{m(C^2+gC)}$			where
λ_2					
$\hat{\mathbf{y}}_{11}\left\{\right.$	$\dfrac{c\sqrt{2km(g+C)}}{D_1}$	$\dfrac{ic\sqrt{2km(g+C)}}{D_1}$	$\dfrac{-2\sqrt{2ikmc}}{D_1}$	$\dfrac{-2\sqrt{2kmc}}{D_1}\left.\right\}$	$D_1 = C\sqrt{\dfrac{C^2-gC}{km}(C^2+gC)}$
$\hat{\mathbf{y}}_{12}\left\{\right.$	$\dfrac{ic\sqrt{2km(g-C)}}{D_2}$	$\dfrac{-c\sqrt{2km(g-C)}}{D_2}$	$\dfrac{-2\sqrt{2kmc}}{D_2}$	$\dfrac{-i2\sqrt{2kmc}}{D_2}\left.\right\}$	$D_2 = C\sqrt{\dfrac{C^2+gC}{km}(C^2-gC)}$

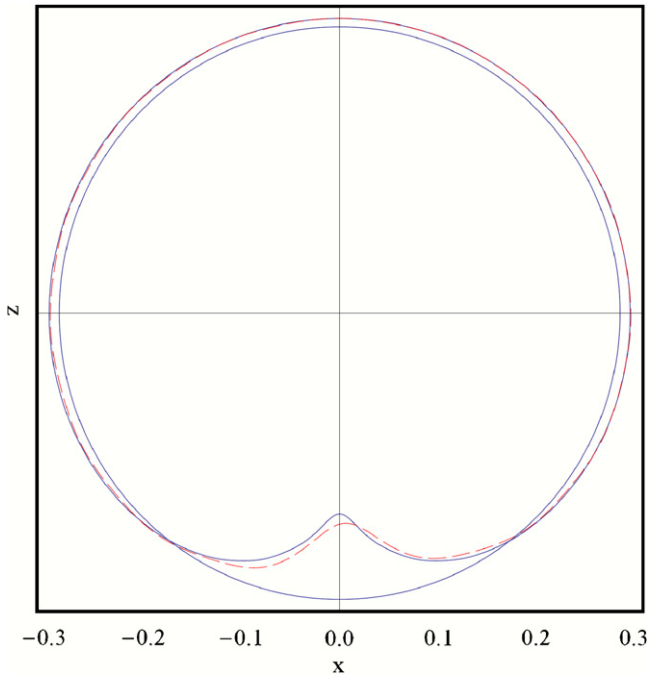

Fig. 6. Schematic of steady deformation (m) configuration, $\Omega = 200$ rad/s: (—), undamped; (- - -), modal damping = 0.1.

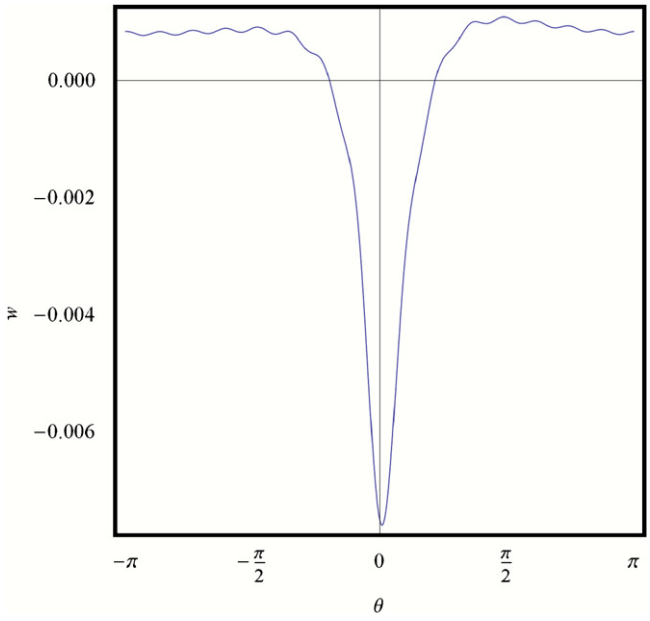

Fig. 7. Steady radial deformation (m) along the circumference (radian), modal damping = 0.1, $\Omega = 200$ rad/s.

the variation of wheel center load behaves like a damped single degree of freedom system (see Fig. 8). The effect of damping on the tire deformation is demonstrated in Figs. 6 and 9. Fig. 10 shows the variation of tire deformation with time; it is observed that after about 0.1 s the tire deformation reaches its steady state in this case.

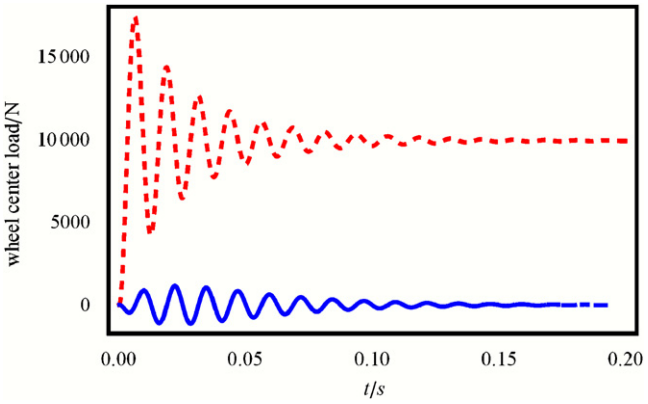

Fig. 8. Variation of tire wheel center load (N) with time (s), modal damping = 0.1, $\Omega = 200$ rad/s: (- - -), vertical force; (—) fore-and-aft force.

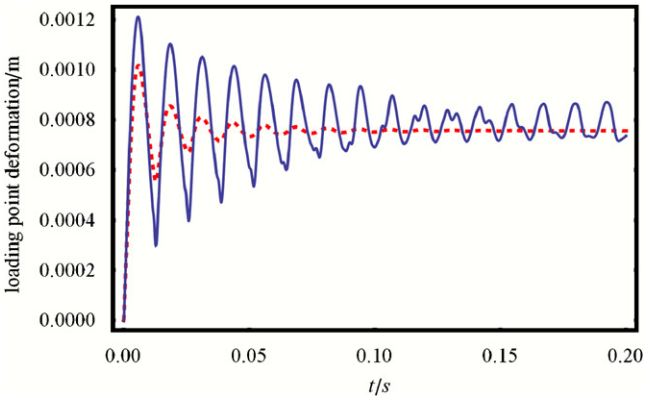

Fig. 9. Variation of radial deformation (m) at loading point with time (s), $\Omega = 200$ rad/s: (—), modal damping = 0.01; (- - -), modal damping = 0.1.

6. Discussions

6.1. Validation of the matrix perturbation theory

To validate the developed matrix perturbation theory for the analysis of damped REF, a direct numerical integration has been performed for Eq. (29). Corresponding to the numerical case in Section 5.3, the generalized force vector $\bar{\mathbf{Q}}$ can be written as

$$\bar{\mathbf{Q}}(t) = \left\{ -10000\frac{n}{\pi r}\sin n(\phi_0 - \Omega t) \quad 10000\frac{n}{\pi r}\cos n(\phi_0 - \Omega t) \quad 0 \quad 0 \right\}^{\mathrm{T}} \tag{37}$$

With the initial conditions $\mathbf{x}(t) = 0$, i.e. $a_n = b_n = \dot{a}_n = \dot{b}_n = 0$, Eq. (29) has been numerically solved to get $a_n, b_n, \dot{a}_n, \dot{b}_n$ up to $n = 30$. The numerical solutions of $a_n, b_n, \dot{a}_n, \dot{b}_n$ from Eq. (29) are then compared with those from matrix perturbation theory, i.e. Eq. (32).

Figs. 11 to 13 show comparisons of modal coordinates of $n = 1$, 10 and 30 from direct numerical integration and matrix perturbation theory respectively. It can be found that the modal coordinates a_n, b_n for all cases match very well, while $\dot{a}_n, \dot{b}_n$ have a very slight difference. Therefore, it can be concluded that the matrix perturbation theory developed in this work is accurate enough for the damped REF model.

Fig. 14 shows the modal coordinates of $n = 1$, 10, in fixed coordinates system, demonstrating the accuracy of the developed method in another way.

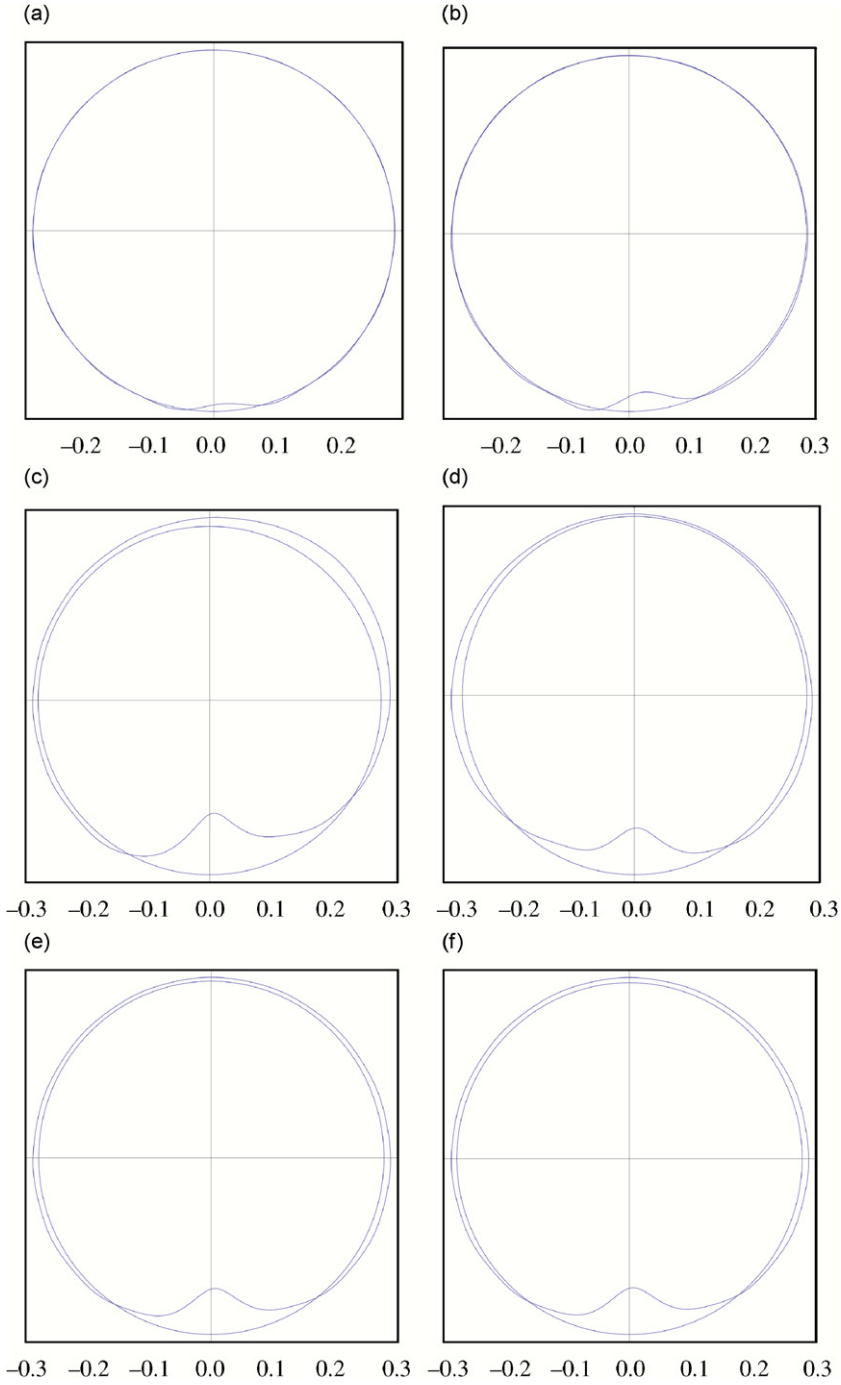

Fig. 10. Variation of tire deformation (m) with time (s): modal damping = 0.1, $\Omega = 200$ rad/s: (a) $t = 0.0005$ s, (b) $t = 0.001$ s, (c) $t = 0.005$ s, (d) $t = 0.01$ s, (e) $t = 0.05$ s, and (f) $t = 0.1$ s.

6.2. Stability analysis

Eq. (32) can be interpreted as a formulation of damped dynamic response under initial conditions, where the the first correction of the eigenvalue λ_{1i} plays the role of damping. Then the stability condition of the system

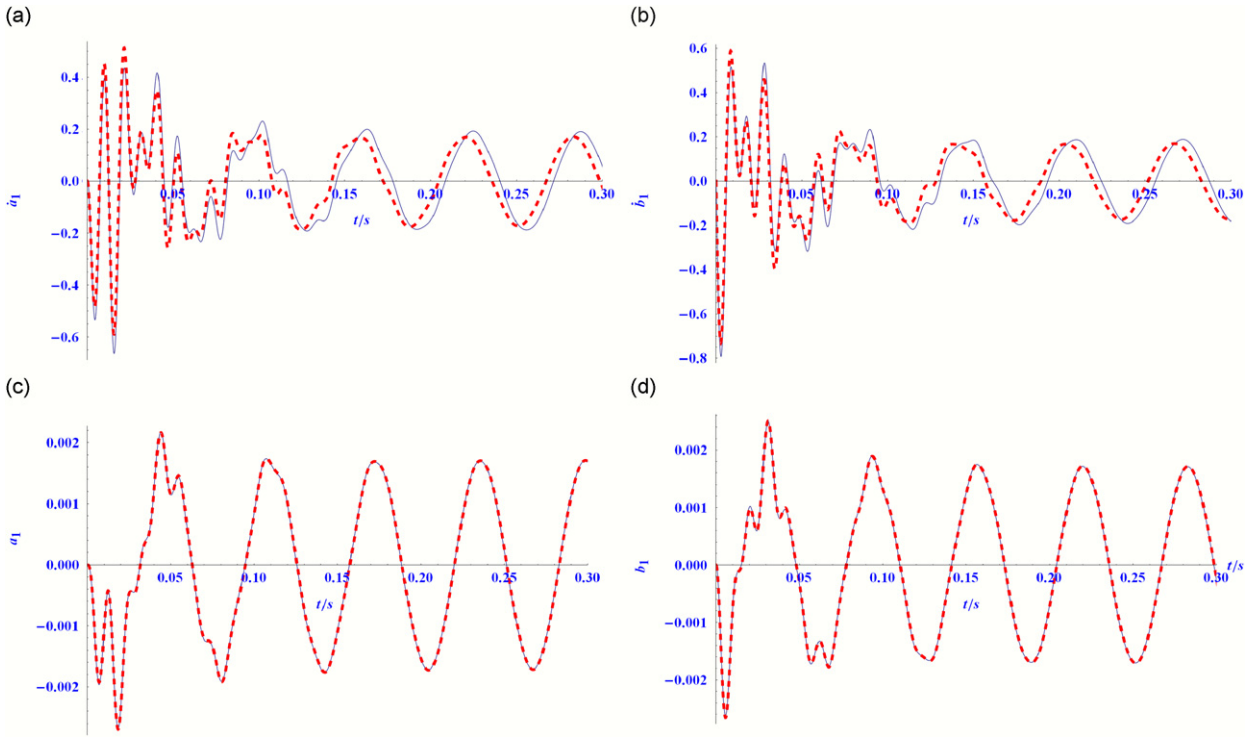

Fig. 11. Comparisons of modal coordinates of $n = 1$, from: (- - -), direct numerical integration; (—), matrix perturbation theory.

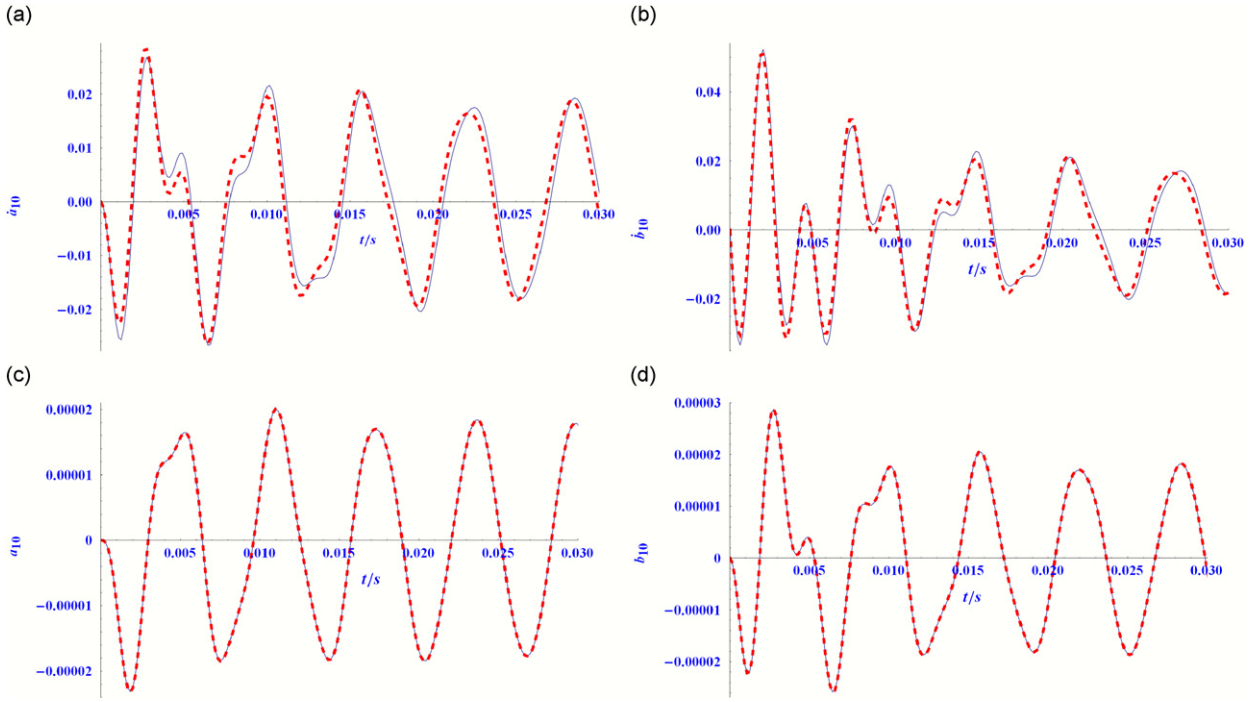

Fig. 12. Comparisons of modal coordinates of $n = 10$, from: (- - -), direct numerical integration; (—), matrix perturbation theory.

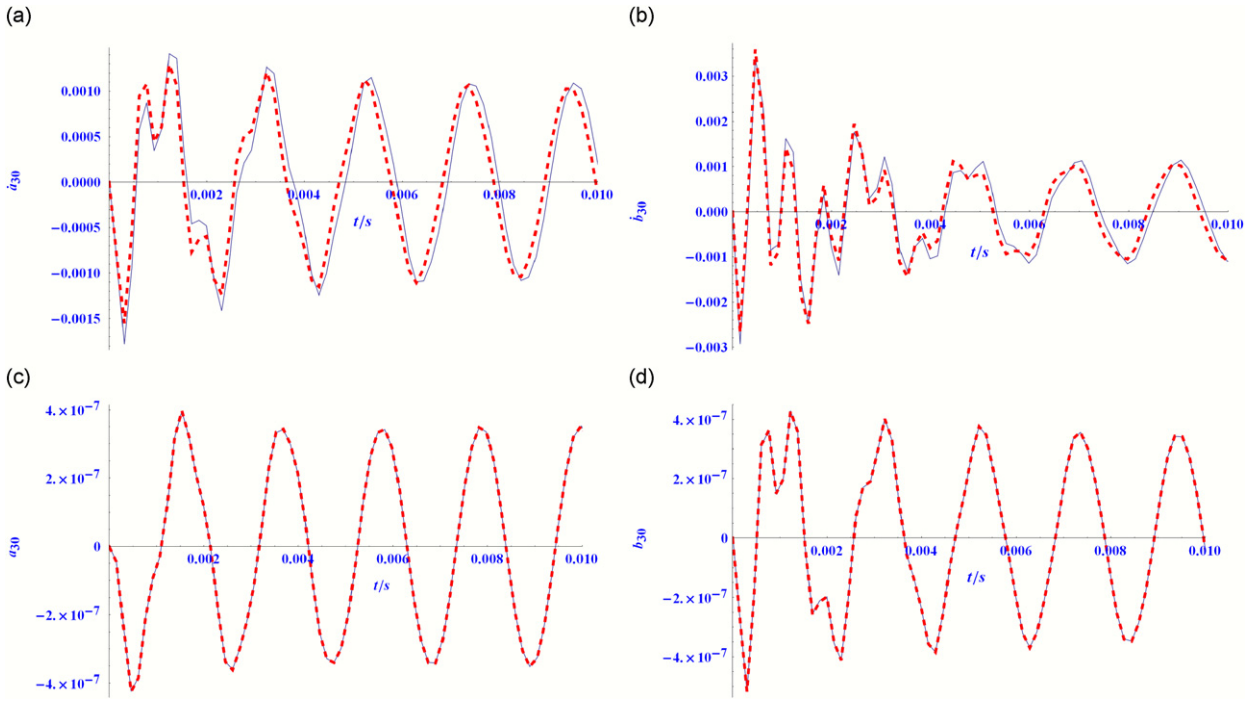

Fig. 13. Comparisons of modal coordinates of $n = 30$, from: (- - -), direct numerical integration; (—), matrix perturbation theory.

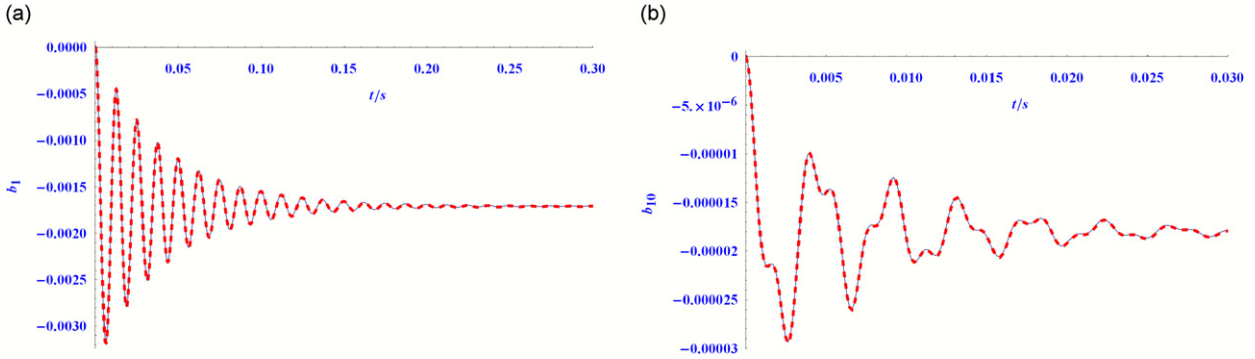

Fig. 14. Modal coordinates in fixed coordinates system: (- - -), direct numerical integration; (—), matrix perturbation theory.

can be written as

$$\lambda_{1i} \leqslant 0 \tag{38}$$

From this stability condition, the critical speed can be derived as

$$\Omega_{\mathrm{cri}} = \sqrt{\frac{EI(-n^2 + 2n^4 - n^6) + p_0 br^3(n^2 - n^4) - r^4(k_v + k_w n^2)}{\rho A r^4(n^4 - 3n^2)}} \tag{39}$$

It is easy to find that for only $n = 1$, Eq. (39) has solution with $\Omega_{\mathrm{cri}} = \omega_1$.

6.3. Potential application of the developed approach

The analytical formulation described in Eq. (32) provides much flexibility in modeling rotating vibration structures such as rolling tires. One advantage of the formulation is that it includes transient response, which

make it possible the real dynamic modeling of rolling tire over cleat or uneven road by REF model [35,36]. Another advantage is that it provides a way to get dynamic flexibility matrix of the tire, based on which the matrix condensation method may be used to solve the dynamic contact response more quickly and efficiently.

7. Summary and conclusions

This paper presents a new analytical formulation of complete forced solution including transient response for the rotating tire REF model. The developed methodology features the application of Meirovitch modal analysis and matrix perturbation theory. Both the steady state and transient responses of rotating tires can be analyzed by using REF model and the proposed approach. By comparison with the direct numerical integration method, it can be seen that the developed theory produces quite accurate results. It is shown that for the damped rotating REF under stationary constant point load, the wheel center load variation behaves like the damped vibration of a single degree of freedom system and converges to the applied load while the displacements at the loading point contain multiple frequencies. The developed theory provides much flexibility in modeling rotating vibration structures such as rolling tires. Incorporating a contact or interface model, the proposed method can be used to understand and model the tire dynamic responses under universal road situations such as an obstacle or a cleat.

Acknowledgments

The first author wishes to express special thanks to AvH foundation of Germany. This paper was supported by the ''National Science Foundation of China'' under Project No. 10202009. The valuable comments and suggestions by the editor and two reviewers are gratefully acknowledged.

References

[1] A. Chiesa, Vibrational performance differences between tires with cross-biased plies and radial plies, SAE Paper 650117, 1965.
[2] F. Böhm, Mechanik des Gurtelreifens, *Ingenicar-Archiv* 35 (1966) 82–101.
[3] G.R. Potts, C.A. Bell, L.T. Charek, T.K. Roy, Tire Vibrations, *Tire Science and Technology* 5 (1977) 202–225.
[4] L.H. Yam, D.H. Guan, A.Q. Zhang, Three-dimensional modal shapes of a tire using experimental modal analysis, *Experimental Mechanics* 40 (2000) 369–375.
[5] D.H. Guan, Experimental modal analysis of tires, *Experimental Techniques* 24 (2000) 39–45.
[6] D.H. Guan, J. Shang, L.H. Yam, Establishment of model for steady state cornering properties using experimental modal parameters, *Vehicle System Dynamics* 34 (2000) 43–56.
[7] S.K. Clark, The rolling tire under load, SAE Paper 650493, 1965.
[8] J.T. Tielking, Plane vibration characteristics of a pneumatic tire model, SAE Paper 650492, 1965.
[9] J. Padovan, On viscoelasticity and standing waves in tires, *Tire Science and Technology* 4 (1976) 233–246.
[10] H.B. Pacejka, Tire in-plane dynamics, in: S.K. Clark (Ed.), *Mechanics of Pneumatic Tires*, Vol. 122, National Bureau of Stands Monograph, Washington, DC, 1971.
[11] W. Soedel, On the dynamic response of rolling tires according to thin shell approximations, *Journal of Sound and Vibration* 41 (1975) 233–246.
[12] K. Yamagishi, J.T. Jenkins, The circumferential contact problem for the belted radial tire, *ASME Journal of Applied Mechanics* 47 (1980) 513–524.
[13] W. Soedel, M.G. Prasad, Calculation of natural frequencied and model of tires in road contact by utilizing eigenvalues of axisymmetric non-contacting tire, *Journal of Sound and Vibration* 70 (1980) 573–584.
[14] L.E. Kung, W. Soedel, T.Y. Yang, On the dynamic response at the wheel axle of a pneumatic tire, *Journal of Sound and Vibration* 107 (1986) 195–213.
[15] L.E. Kung, W. Soedel, T.Y. Yang, Free vibration of pneumatic tire–wheel unit using a ring on an elastic foundation and a finite element method, *Journal of Sound and Vibration* 107 (1986) 181–194.
[16] S.C. Huang, C.K. Su, In-Plane dynamics of tires on the road based on an experimentally verified rolling ring model, *Vehicle System Dynamics* 21 (1992) 247–267.
[17] S.C. Huang, W. Soedel, Effects of coriolis acceleration on the free and forced in-plane vibrations of rotating rings on elastic foundation, *Journal of Sound and Vibration* 115 (1987) 253–274.
[18] Gong Sunrong, A Study of In-plane Dynamics of Tires, PhD Thesis. Delft University of Technology, Faculty of Mechanical Engineering and Marine Technology, 1993.
[19] C.R. Dohrmann, Dynamics of tire–wheel-suspension assembly, *Journal of Sound and Vibration* 210 (1998) 627–642.

[20] S.J. Kim, A.R. Savkoor, Contact problem of in-plane rolling of tires on a flat road, *Vehicle System Dynamics Supplement* 27 (1997) 189–206.
[21] L.E. Kung, Radial vibrations of pneumatic radial tires, SAE Paper 900759, 1990.
[22] L.E. Kung, W. Soedel, T.Y. Yang, Natural frequencies and modal shapes of an automotive tire with interpretation and classification using 3-D computer graphics, *Journal of Sound and Vibration* 102 (1985) 329–346.
[23] A.M. Burke, O.A. Olatunbosun, Contact modeling of the tyre/road surface, *International Journal of Vehicle Design* 18 (1997) 194–202.
[24] Y.B. Chang, T.Y. Yang, W. Soedel, Dynamic analysis of a radial tire by FEM and modal expansion, *Journal of Sound and Vibration* 96 (1983) 1–11.
[25] B. Kao, M. Riesner, P. Surulinarayanasami, Modal analysis of a tire and wheel and its application for vehicle ride evaluation, SAE Paper 860826, 1986.
[26] C.W. Mousseau, G.M. Hulbert, An efficient tire model for the analysis of spindle forces produced by a tire impacting large obstacles, *Computer Methods in Applied Mechanics and Engineering* 135 (1996) 15–34.
[27] T.R. Richards, L.T. Charek, R.W. Scavuzzo, The effects of spindle and patch boundary conditions on tire vibration modes, SAE Paper 860243, 1986.
[28] P.W.A. Zegelaar, Modal analysis of tire in-plane vibration, SAE Paper 971101, 1997.
[29] L. Nasdala, M. Kaliske, A. Becker, H. Rothert, An efficient viscoelastic formulation for steady-state rolling structures, *Computational Mechanics* 22 (1998) 395–403.
[30] P.W.A. Zegelaar, H.B. Pacejka, The in-plane dynamics of tyres on uneven roads, *Vehicle System Dynamics Supplement* 25 (1996) 714–730.
[31] M. Gipser, A new fast tire model for ride comfort simulations, *International Adams Users Conference*, Berlin, Germany, 1999.
[32] L. Meirovitch, A new method of solution of the eigenvalue problem for gyroscopic systems, *AIAA Journal* 12 (1974) 1337–1342.
[33] L. Meirovitch, A modal analysis for the response of linear gyroscopic systems, *Journal of Applied Mechanics* 42 (1975) 446–450.
[34] L. Meirovitch, G. Ryland, Response of slightly damped gyroscopic systems, *Journal of Sound and Vibration* 67 (1979) 1–19.
[35] Y.T. Wei, Modeling of tire rolling contact response by REF Model, SAE Paper Number: 08M-76.
[36] Y.T. Wei, L. Nasdala, H. Rothert, Analysis of tire rolling contact response by REF model, *Tire Science and Technology* 32 (4) (2004) 214–235.